of $[(bpy)_2(O)Ru^{IV}ORu^{V}(O)(bpy)_2]^{3+}$ is an effective electrocatalyst for the oxidation of 2-propanol to acetone. A variety of distinct oxidative mechanistic pathways have been identified for $[(bpy)_2(py)Ru^{IV}(O)]^{2+}$ including examples of O-atom transfer, H-atom transfer, hydride transfer, and ring attack on phenols.[17,19,20] These pathways may also exist for the μ-oxo oxidants, but additional pathways may also appear and the full scope of these reagents remains to be exploited.

Acknowledgment is made to the National Institutes of Health under Grant No. 5-R01-GM32296-05 and to the National Science Foundation under Grant No. CHE-8601604 for support of this research.

(17) (a) Roecker, L.; Meyer, T. J. *J. Am. Chem. Soc.* **1987**, *109*, 746. (b) Meyer, T. J. *J. Electrochem. Soc.* **1984**, *131*, 221C. (d) Thompson, M. S.; Meyer, T. J. *J. Am. Chem. Soc.* **1982**, *104*, 5070.
(18) Raven, S. J.; Meyer, T. J., unpublished results.
(19) (a) Binstead, R. A.; Moyer, B. A.; Samuels, G. J.; Meyer, T. J. *J. Am. Chem. Soc.* **1981**, *103*, 2897. (b) Binstead, R. A.; Meyer, T. J. *J. Am. Chem. Soc.* **1987**, *109*, 3287.
(20) (a) Dobson, J. C.; Seok, W. K.; Meyer, T. J. *Inorg. Chem.* **1986**, *25*, 1614. (b) Roecker, L.; Dobson, J. C.; Vining, W. J.; Meyer, T. J. *Inorg. Chem.* **1987**, *26*, 779. (c) Seok, W. K.; Meyer, T. J. *J. Am. Chem. Soc.*, in press.

Contribution from the Department of Chemistry, University of Alberta, Edmonton, Alberta, Canada T6G 2G2

Kinetics and Products of the Complexation of $(H_2O)_5CrCH_2CN^{2+}$ by Pyrophosphate and Phosphate Ions

M. J. Sisley and R. B. Jordan*

Received April 26, 1988

The kinetics and products of the reactions of phosphate and pyrophosphate ions with $(H_2O)_5CrCH_2CN^{2+}$ have been studied in aqueous acid. In both cases, the reaction proceeds in three discernible stages. The first step on the stopped-flow time scale is assigned to displacement of the water trans to the alkyl ligand with rate constants (M^{-1} s^{-1}, 25 °C, 1.00 M $NaClO_4/HClO_4$) of 0.63 ($H_2P_2O_7^{2-}$), 0.50 ($H_3P_2O_7^-$), 0.47 ($H_2PO_4^-$), and 0.07 (H_3PO_4). The kinetics also yield equilibrium constants for this step of 15 and 3.1 M^{-1} for $H_2P_2O_7^{2-}$ and $H_2PO_4^-$, respectively. The second stage is attributed to isomerization from the trans to the cis position with rate constants of 1.4×10^{-3}, 5.3×10^{-4}, and 1.1×10^{-3} s^{-1} for the $H_2P_2O_7^{2-}$, $H_3P_2O_7^-$, and $H_2PO_4^-$ complexes, respectively. This is followed by a rapid second anation, and finally the bis complex loses its alkyl group with measurable rate constants of 2×10^{-4} and 6×10^{-4} s^{-1} for the pyrophosphate and phosphate systems, respectively. The expected products after the first and last stages have been separated by ion-exchange chromatography and characterized by their electronic spectra. The results are compared to those of previous studies.

Introduction

A number of studies have shown that pentaaquachromium(III) alkyl complexes undergo remarkably rapid reactions with nucleophiles as shown in eq 1. These results have been summarized

$$(H_2O)_5CrCH_2CN^{2+} + X \rightarrow (H_2O)_4(X)CrCH_2CN^{2+} \quad (1)$$

in a recent review.[1] This reactivity has been associated with the trans effect of the alkyl ligand.

In the past 2 years, we have observed that $(H_2O)_5CrCH_2CN^{2+}$ reacts with nucleophiles such as oxalate[2] and hypophosphite[3] to give further substitution coupled with isomerization and chelation in the case of oxalate. The present work was undertaken to explore the reactivity patterns for these processes with phosphate and pyrophosphate as nucleophiles. It is also possible that the results might be relevant to the general coordination chemistry and preparative methods for chromium(III) complexes of phosphate, pyrophosphate, and derivatives such as AMP and ADP.[4,5]

Results

Spectrophotometric Observations and Products with Pyrophosphate. The reaction of $(H_2O)_5CrCH_2CN^{2+}$ with excess pyrophosphate in dilute aqueous acid proceeds in at least three stages, which are discernible from changes in the electronic spectrum. The initial change on the stopped-flow time scale causes a general increase in absorbance with the largest change at ~355 nm. This is followed by a small absorbance increase at the 408-nm peak of the reactant. Within about 10 min, there is a much larger decrease in absorbance at 408 nm with a shift in the maximum to longer wavelength. An isosbestic point is retained at ~485 nm for ~20 min, but this is lost and a new isosbestic point near 605 nm persists after ~1 h until the end of the reaction. During the slower stages, the 525-nm maximum of the reactant disappears and a new peak appears near 625 nm.

The final product solution is apple green, and the electronic spectrum (Table I) corresponds to that of the bis(pyrophosphato)chromium(III) complex reported by DePamphilis and Cleland.[6] This shows that the $-CH_2CN$ ligand has been lost during the overall process. The final product was separated from

Table I. Visible Region Electronic Spectra of Chromium(III) Complexes

complex	wavelength, nm (molar absorptivity, M^{-1} cm^{-1})		sh wavelength, nm	ref
$(H_2O)_5CrCH_2CN^{2+}$	408 (102)	525 (40.1)		*a*
$(H_2O)_5Cr(PO_4H_2)^{2+}$	417 (17.9)	590 (17.3)		*a, b*
$(H_2O)_5Cr(PO_4H_2)^{2+}$	416 (17.2)	591 (16.0)	640, 670	*a, c*
$(H_2O)_5Cr(PO_4H_2)^{2+}$	417 (17.7)	591 (17.1)	640, 670	*a, d*
$(H_2O)_4Cr(PO_4H_2)_2^+$	425 (18.8)	605 (18.3)	640, 675	*a, e*
$(H_2O)_4Cr(PO_4H_2)_2^+$	433 (23.1)	609 (22.4)	644, 678	*a, f*
$(H_2O)_5Cr(P_2O_7H_2)^+$	417 (18.0)	593 (17.1)		*a, g*
$(H_2O)_5Cr(P_2O_7H)$	424 (22.4)	594 (22.7)		*h*
$(H_2O)_5Cr(P_2O_7H)$	425 (25.0)	595 (24.0)		*i*
$(H_2O)_4Cr(P_2O_7H_2)_2^-$	441 (20.8)	624 (20.0)	650, 680	*a, j*
$(H_2O)_4Cr(P_2O_7H_2)_2^-$	441 (21)	626 (20)	650, 680	*k*

[a] This work. [b] The 2+ product after 75 s and treatment with Hg(II). [c] Product from Cr(II) and $(NH_3)_4CoPO_4$. [d] The 2+ product after 102 min and treatment with Hg(II). [e] The <2+ product after 102 min and treatment with Hg(II). [f] Solid dissolved in 0.01 M perchloric acid. [g] The 2+ product after 90 s and treatment with Hg(II), in 0.01 M perchloric acid. [h] As in footnote *g*, except pH 5.5. [i] Reference 9. [j] Final product in ~0.01 M perchloric acid. [k] Reference 6.

(1) Espenson, J. H. *Adv. Inorg. Bioinorg. Mech.* **1982**, *1*, 1.
(2) Sisley, M. J.; Jordan, R. B. *Inorg. Chem.* **1987**, *26*, 273.
(3) Sisley, M. J.; Jordan, R. B. *Inorg. Chem.* **1987**, *26*, 2833.
(4) Cleland, W. W. *Methods Enzymol.* **1982**, *87*, 159.
(5) Lin, I.; Dunaway-Mariano, D. *J. Am. Chem. Soc.* **1988**, *110*, 950 and references therein.
(6) DePamphilis, M. L.; Cleland, W. W. *Biochemistry* **1973**, *12*, 3714.

0020-1669/88/1327-4483$01.50/0

Table II. Stopped-Flow Kinetic Results for the Reaction of Pyrophosphate ($H_nP_2O_7^{4-n}$) with $(H_2O)_5CrCH_2CN^{2+}$ [a] (1 M $NaClO_4/HClO_4$ at 25 °C)

$[H_nP_2O_7^{4-n}]_{tot}$, M	$[H^+]_{tot}$, M	$10[H^+]_{free}$,[b] M	$10[H_2P_2^{2-}]$,[b] M	$10[H_3P_2^-]$,[b] M	10(rate const), s^{-1}	
					obsd	calcd[c]
0.0250	0.0660	0.102	0.197	0.0500	0.638	0.623
0.0500	0.121	0.101	0.394	0.100	0.772	0.772
0.100	0.232	0.101	0.788	0.200	1.03	1.07
0.150	0.344	0.103	1.178	0.305	1.40	1.37
0.200	0.454	0.100	1.582	0.396	1.67	1.67
0.100	0.326	0.502	0.382	0.482	1.10	1.08
0.0250	0.177	0.999	0.0510	0.128	0.800	0.792
0.100	0.409	1.00	0.202	0.510	1.05	1.08
0.200	0.717	1.00	0.405	1.020	1.45	1.46
0.0250	0.285	2.00	0.0210	0.108	0.883	0.864
0.100	0.540	2.00	0.0850	0.430	1.07	1.07
0.200	0.880	2.00	0.171	0.861	1.46	1.34

[a] Measured at 355 nm with $[CrCH_2CN^{2+}] = (4.5–5.0) \times 10^{-3}$ M. [b] Calculated from the total $HClO_4$ and $Na_2H_2P_2O_7$ added using $K_{a_1} = 0.178$ M and $K_{a_2} = 3.98 \times 10^{-2}$ M. [c] Calculated from a least-squares fit to eq 2.

pyrophosphate by following the procedure of DePamphilis and Cleland.[6] Analysis for chromium and pyrophosphate[7] gave a ratio of $(H_nP_2O_7^{4-n})$:Cr = 1.95:1, which supports the proposed formulation.

The intermediate product after the stopped-flow reaction was difficult to isolate because of its kinetic lability. Therefore, it was necessary to add Hg(II) to dealkylate the chromium before product separation. The details of the dealkylation reaction have been discussed previously.[3,8] A solution containing 0.10 M total $H_nP_2O_7^{n-4}$, 2×10^{-3} M $(H_2O)_5CrCH_2CN^{2+}$, and 0.01 M free H^+ in 30 mL of water was allowed to react for 90 s, and then 4 mL of 0.5 M $Hg(ClO_4)_2$ was added to quench the reaction by dealkylating the chromium. The mixture was filtered to remove $Hg(H_2P_2O_7)$ and subjected to ion-exchange chromatography at 4 °C on Dowex 50W-X12 (H^+). A pale green solution passed directly through the resin while 3+ and 4+ ($CrNCCH_2Hg^{4+}$) fractions were absorbed.

The electronic spectrum (Table I) of the pale green product shows no change over 1 h in 0.05 M $HClO_4$. When the pH of the solution is adjusted to 5.5 with 4 M NaOH, there are increases in absorbance and slight shifts of the maxima to longer wavelengths (Table I). The spectrum at pH 5.5 is quite similar to that of $(H_2O)_4Cr(P_2O_7H)$ reported by Merritt et al.[9] The small differences may be due to free pyrophosphate in our solutions or to a pH difference because the pH is not specified by Merritt et al.

The overall picture from these results is that the fastest reaction produces the monopyrophosphato complex, either monodentate or chelate, and the slower stages are associated with bis(pyrophosphato) complex formation and dealkylation.

Spectrophotometric Observations and Products with Phosphate. The reaction of $(H_2O)_5CrCH_2CN^{2+}$ with phosphate in aqueous acid shows three obvious stages when monitored spectrophotometrically. On the stopped-flow time scale, there are small increases in absorbances and shifts (~2 nm) to longer wavelengths at the absorbance maxima of the reactant. Over the next 1–2 h, the absorbance around 525 nm continues to rise while that at 410 nm decreases and the maxima continue to shift to lower energies. During the final stage, the absorbance decreases around 410 and 525 nm. There appears to be an isosbestic point around 607 nm during the last stage.

The final solution is green with the electronic spectrum given in Table I. The Cr–C bond appears to have been lost since the characteristic maximum at ~400 nm has disappeared.

The product at the end of the first stage was characterized by allowing a solution of 2×10^{-3} M $(H_2O)_5CrCH_2CN^{2+}$ to react with 0.20 M total phosphate in 0.08 M free H^+ for 75 s. Then $Hg(ClO_4)_2$ was added and the solution was kept for 7 h at ambient temperature to allow species such as $(H_2O)_4(H_2PO_4)$-$CrNCCH_2Hg^{3+}$ and $(H_2O)_5CrNCCH_2Hg^{4+}$ to lose the nitrile function by aquation.[8] The solution was then filtered to remove $HgHPO_4$ and ion-exchanged on Dowex 50W-X2 (H^+). Four products could be separated and characterized by charge type. The amounts as a percentage of total chromium are as follows: <2+, 2.7%; 2+, 14.5%; 3+, 77.9%; 4+, 3.1%. The 3+ products is $Cr(OH_2)_6^{3+}$ on the basis of its electronic spectrum. The spectrum of the 2+ product (Table I) indicates that it is $(H_2O)_5Cr(H_2PO_4)^{2+}$ on the basis of a comparison to the spectrum of the product of the reaction of Cr(II) and $Co(NH_3)_4PO_4$ (Table I). Analysis[7] gave a PO_4:Cr ratio of 0.99:1 for the 2+ product, consistent with the proposed formulation.

Scheme I

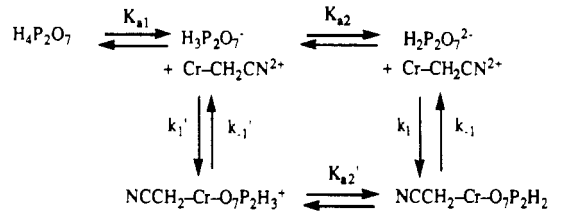

The products after 102 min were determined in the same way. The product distribution is as follows: <2+, 9.5%; 2+, 27.1%; 3+ and 4+, 57.3%. The 2+ species has the same spectrum as that identified after the first stage of reaction (Table I).

The final reaction product after 20 h does not bind to cation-exchange resin and is green. The spectrum in ~0.05 M H^+ is given in Table I. The solid bis(phosphato)chromium(III) complex was prepared as described in the Experimental Section. Analysis[7] of the solid gave a ratio of PO_4:Cr = 2.08:1, and the spectrum of the solid dissolved in aqueous acid is given in Table I. The similarity of this spectrum to that of the final reaction product serves to identify the latter as $(H_2O)_4Cr(H_2PO_4)_2^+$, although they could be different geometrical isomers or mixtures of these isomers.

Stopped-Flow Kinetics with Pyrophosphate. The kinetic results under pseudo-first-order conditions with $[H_nP_2O_7^{n-4}] \gg [CrCH_2CN^{2+}]$ are summarized in Table II. The kinetic observations can be explained by the reactions shown in Scheme I, which predict that the pseudo-first-order rate constant (k_{obsd}) is given by eq 2, where $[H_nP_2O_7^{n-4}]_{tot} = [H_4P_2O_7] + [H_3P_2O_7^-] +$

$$k_{obsd} = (k_1'K_{a_1}[H^+] + k_1K_{a_1}K_{a_2}) \times \left\{ \frac{[H_nP_2O_7^{n-4}]_{tot}}{K_{a_1}K_{a_2} + K_{a_1}[H^+] + [H^+]^2} + \frac{K_{a_2}'}{K_{a_1}K_{a_2}K_f(K_{a_2}' + [H^+])} \right\} \quad (2)$$

$[H_2P_2O_7^{2-}]$, $K_f = k_1/k_{-1}$, and K_{a_1} and K_{a_2} are 0.178×10^{-2} and 3.98×10^{-2} M, respectively.[10] A least-squares analysis gives $k_1 = 0.63 \pm 0.035$ M^{-1} s^{-1}, $k_1' = 0.50 \pm 0.043$ M^{-1} s^{-1}, $K_f = 14.8$

(7) Douglas, L. A.; Field, J. F. B. *Anal. Lett.* **1975**, *8*, 195.
(8) Sisley, M. J.; Jordan, R. B. *Inorg. Chem.* **1986**, *25*, 3547.
(9) Merritt, E. A.; Sundaralingnam, M.; Dunaway-Mariano, D. *J. Am. Chem. Soc.* **1981**, *103*, 3565.
(10) Bottari, E.; Ciavatta, L. *Inorg. Chim. Acta* **1968**, *2*, 74.

Table III. Stopped-Flow Kinetic Results for the Reaction of Phosphate with $(H_2O)_5CrCH_2CN^{2+}$ [a] (1 M $NaClO_4/HClO_4$ at 25 °C)

$[PO_4]_{tot}$, M	$[H^+]_{tot}$, M	$10[H^+]_{free}$, [b] M	$10[H_2PO_4^-]$, [b] M	rate const, s^{-1}	
				obsd [c]	calcd [d]
0.117	0.311	1.94	0.594	0.207	0.205
0.233	0.564	1.18	1.47	0.235	0.240
0.233	0.609	2.17	1.12	0.246	0.237
0.233	0.609	2.17	1.12	0.243	0.237
0.233	0.719	7.11	0.511	0.250	0.267
0.467	1.21	2.35_5	2.14_5	0.303	0.296
0.642	1.55	1.30	3.89	0.350	0.367
0.642	1.66	2.43_5	2.89_5	0.335	0.339
0.642	1.89	8.56	1.22	0.355	0.339
0.817	2.11	2.47	3.66	0.402	0.382
0.817	2.11	2.47	3.66	0.376	0.382

[a] Determined at 410 nm with $[CrCH_2CN^{2+}] = (1.7–2.4) \times 10^{-3}$ M. [b] Calculated with $K_{a_1} = 2.0 \times 10^{-2}$ M. [c] Each value is the average of 10–14 runs with a typical standard deviation on the average of 5%. [d] Calculated from a least-squares fit to eq 3.

Scheme II

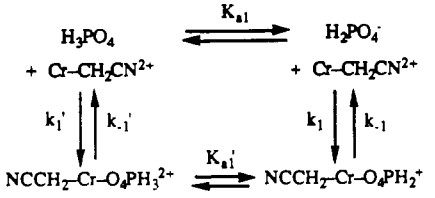

$\pm$ 1.4 M^{-1}, and $K_{a_2}' = 0.12 \pm 0.026$ M.[11] The observed and calculated values are compared in Table II.

Stopped-Flow Kinetics with Phosphate. The kinetic observations under pseudo-first-order conditions are summarized in Table III. The results are consistent with the reactions in Scheme II. This scheme predicts that, if $K_{a_1}' \gg [H^+]$, then the observed pseudo-first-order rate constant is given by eq 3, where $K_f = k_1/k_{-1}$ and

$$k_{obsd} = (k_1'[H^+] + k_1K_{a_1})\left\{\frac{[PO_4]_{tot}}{K_{a_1} + [H^+]} + \frac{1}{K_{a_1}K_f}\right\} \quad (3)$$

$[PO_4]_{tot} = [H_3PO_4] + [H_2PO_4^-]$ since HPO_4^{2-} has been ignored because it is a very minor species[12] under the acidic conditions of this study. A least-squares analysis gives $k_1' = (6.8 \pm 1.1) \times 10^{-2}$ M^{-1} s^{-1}, $k_1 = 0.47 \pm 0.03$ M^{-1} s^{-1}, and $K_f = 3.1 \pm 0.3$ M^{-1}. The observed and calculated values are compared in Table III.

Kinetics of the Slower Reactions with Pyrophosphate. These reactions were monitored at 410 and 609 nm. As noted above, 609 nm is close to an isosbestic point for the slowest reaction. Typical absorbance–time plots are shown in Figure 1. The data at 609 nm can be fitted satisfactorily to a single-exponential decay, but at 410 nm a double-exponential model is required because the absorbance change is slower during the first 1000–2000 s. The larger absorbance change at 410 nm indicates that the alkyl group is being lost, but there must be a preceding reaction that causes the absorbance–time curves to be flatter initially.

The data at 609 nm were analyzed by least squares to obtain the observed pseudo-first-order rate constant γ_1. Then the 410-nm data were fitted to eq 4 to obtain γ_2 with γ_1 fixed at the value

$$A_t = A_\infty + X_1 \exp(-\gamma_1 t) + X_2 \exp(-\gamma_2 t) \quad (4)$$

obtained at 609 nm under the same experimental conditions. This analysis gave excellent fits of the data as can be seen from the calculated curves in Figure 1. The values of γ_1 and γ_2 are given in Table IV.

(11) The errors are 1 standard deviation and the 95% confidence limits are about 3 times larger. Significant figures beyond those indicated by the error limits are retained in order to avoid roundoff in the calculated values.

(12) Martell, A. E.; Smith, R. M. *Critical Stability Constants*; Plenum Press: New York, 1982; Vol. 5, p 407.

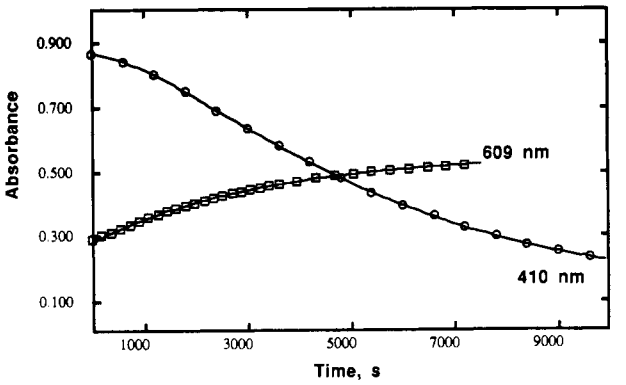

Figure 1. Variation of absorbance with time for the reaction of pyrophosphate (0.025 M total) with $(H_2O)_5CrCH_2CN^{2+}$ in 0.010 M free H^+ at 409 nm (○) and at 609 nm (□). The data at 609 nm are fitted to a single-exponential model while those at 410 nm are fitted to a two-exponential model with the larger rate constant equal to that from 609 nm.

Table IV. Kinetic Results for the Second and Third Stages of the Reaction of Pyrophosphate with $(H_2O)_5CrCH_2CN^{2+}$ [a] (1.0 M $NaClO_4/HClO_4$ at 25 °C)

$[PO_4]_{tot}$, M	$[H^+]_{free}$, M	10^4(rate const), s^{-1}			
		γ_1 [b]		γ_2 [c]	
		obsd	calcd	obsd	calcd
0.0250	0.0100	2.94	3.23	4.06	4.09
0.0500	0.0100	5.00	5.18	4.85	4.89
0.0500	0.1000	2.17	2.20	1.19	1.28
0.0500	0.180	1.54	1.39	0.775	0.785
0.100	0.0100	7.83	7.48	7.05	5.42
0.100	0.100	3.30	3.60	1.69	1.69
0.100	0.180	2.34	2.40	1.28	1.17
0.150	0.0100	10.0	8.77	5.26	5.63
0.200	0.0100	9.67	9.59	5.36	5.73
0.200	0.100	5.83	5.29	1.96	2.01
0.200	0.180	3.60	3.75	1.60	1.55

[a] $[CrCH_2CN^{2+}] = (3.5–4.5) \times 10^{-3}$ M. [b] Determined at 609 nm from a single-exponential fit. [c] Determined at 410 nm from a double-exponential fit to eq 4 with γ_1 fixed at the value from 609 nm.

The dependence of γ_1 and γ_2 on pyrophosphate and hydrogen ion concentrations can be explained by the reactions in Scheme III. This scheme is based on previous experience with hypophosphite and oxalate and also incorporates the irreversible loss of the alkyl group in the final step. The fastest reaction is treated as a rapid preequilibrium.

In general, the reactions in Scheme III can be represented by

$$A \underset{\beta_1}{\overset{\kappa_1}{\rightleftharpoons}} B \xrightarrow{\kappa_2} C \quad (5)$$

in which case

$$\gamma_{1,2} = \frac{b \pm (b^2 - 4c)^{1/2}}{2} \quad (6)$$

where $b = \kappa_1 + \beta_1 + \kappa_2$ and $c = \kappa_1\kappa_2$ and

$$\kappa_1 = \frac{(k_2'K_{a_2}[H_3P_2] + k_2K_{a_2}'[H_2P_2])K_f}{K_{a_2}' + K_f(K_{a_2}'[H_2P_2] + K_{a_2}[H_3P_2])}$$

$$\beta_1 = \frac{(k_{-2}'[H^+] + k_{-2}K_{a_2}'')K_{a_3}}{K_{a_3}(K_{a_2} + [H^+]) + K_{f_2}K_{a_2}''(K_{a_3} + [H^+])[H_2P_2]} \quad (7)$$

$$\kappa_2 = \frac{(k_3'[H^+] + k_3K_{a_3})K_{f_2}K_{a_2}''[H_2P_2]}{K_{a_3}(K_{a_2}'' + [H^+]) + K_{f_2}K_{a_2}''(K_{a_3} + [H^+])[H_2P_2]}$$

where $H_2P_2 \equiv H_2P_2O_7^{2-}$ and $H_3P_2 \equiv H_3P_2O_7^-$. The number of variables can be reduced by noting that $k_{-2}' = K_{a_2}''k_2'k_{-2}/K_{a_2}'k_2$.

Preliminary analysis revealed that $\beta_1 \ll \kappa_1, \kappa_2$ so that $b = \kappa_1 + \kappa_2$ and then $\gamma_1 = \kappa_1$ and $\gamma_2 = \kappa_2$. Since $(\kappa_1 - \kappa_2)^2 = (\kappa_2 - \kappa_1)^2$, it is also possible that $\gamma_1 = \kappa_2$ and $\gamma_2 = \kappa_1$, a feature that has been

Scheme III

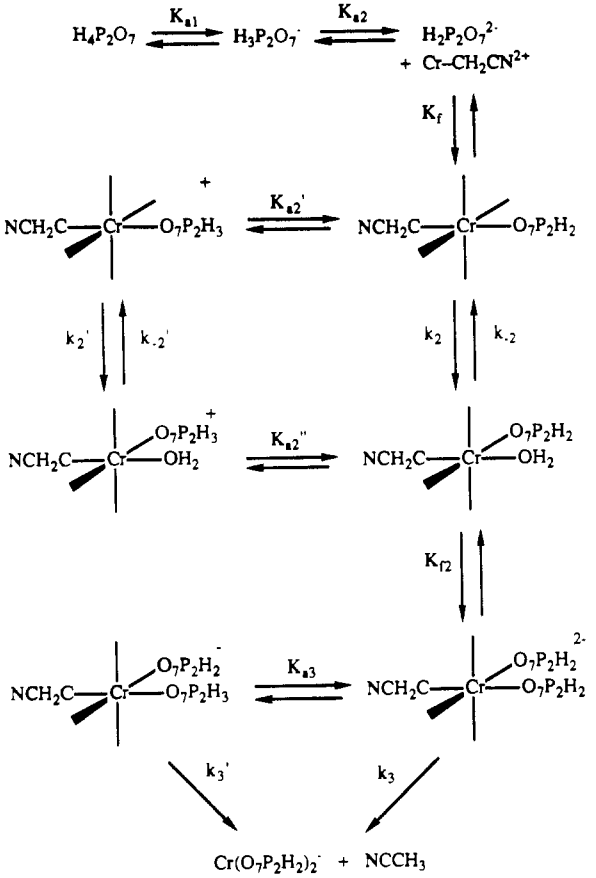

noted previously for such systems.[13] In this case, the separation has been made on the basis of observations at two wavelengths so that the former assignment can be made.

A least-squares analysis of the values of γ_1 gives $k_2' = (1.4 \pm 0.06) \times 10^{-3}$ s^{-1}, $k_2 = (5.30 \pm 0.16) \times 10^{-4}$ s^{-1}, and $K_{a_2}' = 0.112 \pm 0.06$ M.[11] The last value is in excellent agreement with that of 0.12 M obtained from the stopped-flow study.

The least-squares best fit of the γ_2 values is obtained with the limiting form of eq 6 when $[H^+] > K_{a_2}''$, K_{a_3}, in which case

$$\gamma_2 = \kappa_2 = \frac{(k_3'[H^+] + k_3K_{a_3})[H_2P_2]}{[H^+]\left(1 + \frac{K_{f_2}K_{a_2}''}{K_{a_3}}[H_2P_2]\right)} \frac{K_{f_2}K_{a_2}''}{K_{a_3}} \qquad (8)$$

The least-squares best-fit values from eq 7 are $k_3K_{a_3} = (4.0 \pm 0.3) \times 10^{-6}$ M^{-1} s^{-1}, $k_3' = (2.1 \pm 0.3) \times 10^{-4}$ s^{-1}, and $K_{f_2}K_{a_2}''/K_{a_3} = (1.04 \pm 0.24) \times 10^2$ M^{-1}.[11] The observed and calculated values of γ_1 and γ_2 are compared in Table IV.

It is not surprising that $[H^+] > K_{a_3}$ as required by eq 7, because the larger negative charge and potential for intramolecular hydrogen bonding (see I) could make $NCCH_2Cr(H_2P_2)(H_3P_2)^-$ a much weaker acid than $NCCH_2Cr(H_3P_2)^+$. But it does seem

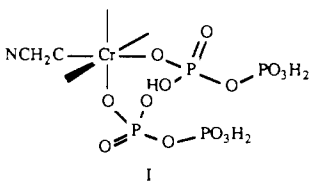

I

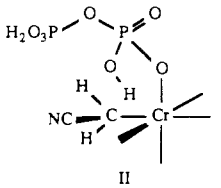

II

unexpected that K_{a_2}'' would be much smaller than K_{a_2}' since they refer to the same process in cis and trans isomers. If K_{a_2}'' is fixed at 0.02 M, then the fit of the γ_2 values to eq 6 has a 30% larger

(13) Buckingham, D. A.; Francis, D. J.; Sargeson, A. M. *Inorg. Chem.* **1974**, *13*, 2630.

Table V. Kinetic Results for the Second and Third Stages of the Reaction of Phosphate with $(H_2O)_5CrCH_2CN^{2+}$ [a] (1.0 M $NaClO_4/HClO_4$ at 25 °C)

$[PO_4]_{tot}$, M	$[H^+]_{tot}$, M	$10^2 \times [H^+]_{free}$, M	$10^2 \times [H_2PO_4^-]$, M	10^4(rate const), s^{-1}			
				γ_1 [b]		γ_2 [c]	
				obsd	calcd	obsd	calcd
0.117	0.310	1.91	5.99	2.50	2.56	0.172	0.205
0.175	0.425	1.14	11.1	3.84	3.62	0.439	0.424
0.175	0.552	6.73	4.01	1.95	2.07	0.124	0.122
0.233	0.610	2.20	11.1	3.54	3.62	0.430	0.422
0.350	0.845	1.22	21.7	5.11	5.16	0.861	0.843
0.350	0.910	2.29	16.3	4.43	4.46	0.656	0.636
0.350	1.054	7.65	7.25	2.84	2.85	0.285	0.259
0.467	1.210	2.36	21.5	5.20	5.13	0.816	0.834
0.583	1.510	2.44	26.3	5.60	5.66	1.03	1.01
0.700	1.685	1.28	42.7_5	6.94	6.92	1.46	1.53
0.700	1.810	2.45	31.4_5	5.94	6.13	1.18	1.18
0.700	2.059	8.83	12.9	4.03	3.94	0.557	0.499

[a] $[CrCH_2CN^{2+}] = (3.6–4.2) \times 10^{-3}$ M. [b] Determined at 607 nm and calculated from a two-exponential fit with one rate constant fixed at the value of γ_2. [c] Determined at 410 nm from a one-exponential fit.

Scheme IV

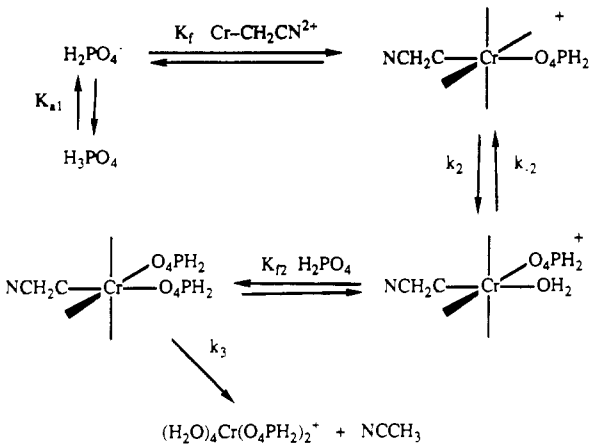

standard deviation than the best fit to eq 7. This seems to place an upper limit on K_{a_2}'' in the range of 0.01–0.02 M or 5–10 times less than K_{a_2}'. It might have been expected that a weaker chromium–pyrophosphate bond in the trans position would make K_{a_2}' smaller than K_{a_2}''. Possibly there is some interaction between the cis alkyl and pyrophosphate ligands, as suggested in II, which makes the cis H_3P_2 a weaker acid.

A discussion of the values of k_2, k_2', k_3, and k_3' will be deferred to the final section.

Kinetics of the Slower Reactions with Phosphate. At 410 nm, only the last stage produces a significant absorbance change. The absorbance–time data at 410 nm are well fitted by a single-exponential decay, and the observed rate constants (γ_2) are given in Table V.

At 607 nm, the dominant process is the second stage; however, the absorbance–time data cannot be satisfactorily fitted to a single-exponential model. Excellent fits were obtained with a two-exponential model (eq 4) with γ_2 fixed at the value under the same conditions at 410 nm. The values of γ_1 also are given in Table V.

The analysis of the values of γ_1 and γ_2 follows that used above for pyrophosphate and is based on the reactions in Scheme IV.

The $\gamma_{1,2}$ values are given by eq 6 with $b = \kappa_1 + \beta_1 + \kappa_2 + \beta_2$ and $c = \kappa_1\kappa_2 + \beta_2(\kappa_1 + \kappa_2)$, where

$$\kappa_1 = \frac{k_2K_f[H_2PO_4^-]}{K_f[H_2PO_4^-] + 1} \qquad \kappa_2 = \frac{k_3K_{f_2}[H_2PO_4^-]}{K_{f_2}[H_2PO_4^-] + 1}$$

$$\beta_1 = \frac{k_{-2}}{K_{f_2}[H_2PO_4^-] + 1} \qquad \beta_2 = k_{-3} \qquad (9)$$

The variations of γ_1 and γ_2 with $[H_2PO_4^-]$ were fitted simultaneously to the above model with $K_f = 3.1$ M as determined

Table VI. Summary of Kinetic Results for Reaction of Several Ligands with $(H_2O)_5CrCH_2CN^{2+}$ (1 M Ionic Strength, 25 °C)

ligand	k_1, k_1', M^{-1} s^{-1}	k_2, k_2', s^{-1}	k_3, k_3', s^{-1}	K_{f_1}, M^{-1}	K_{f_2}, M^{-1}
$H_2P_2O_7^{2-}$	0.63	5.3×10^{-4}	$(4 \times 10^{-6})^a$	14.8	*b*
$H_3P_2O_7^-$	0.50	1.4×10^{-3}	2.1×10^{-4}		
$H_2PO_4^-$	0.47	1.08×10^{-3}	6.4×10^{-4}	3.1	0.88
H_3PO_4	0.068				
$H_2PO_2^{-c}$	0.19	3×10^{-4}		5.45	5.4
$H_3PO_2^c$	0.081				
$HO_2CCO_2^{-d}$	1.6	2.8×10^{-2e}		2.5	

[a] This is the value of $k_3K_{a_3}$; see text for estimate of k_3. [b] See text for an estimate of this value. [c] Reference 2. [d] Reference 3. [e] Rate constant for chelate ring closing.

from the stopped-flow study. The value of β_2 was too small to evaluate, as expected if the last step is loss of the alkyl group. The analysis gives $k_2 = (1.08 \pm 0.04) \times 10^{-3}$ s^{-1}, $k_{-2} = (8.3 \pm 1.1) \times 10^{-5}$ s^{-1}, $k_3 = (6.4 \pm 1.7) \times 10^{-4}$ s^{-1}, and $K_{f_2} = 0.87_5 \pm 0.28$ M^{-1}.[11] The calculated and observed values of γ_1 and γ_2 are compared in Table V.

Discussion

Related kinetic and equilibrium constant results from this and previous studies are summarized in Table VI. The rate constants for the first anation step (k_1, k_1') are not as constant as one might hope for a limiting dissociative mechanism since they range from 0.19 to 1.6 for the oxyanions and are somewhat smaller for the neutral species. The latter effect is expected for the intermediacy of an ion pair. The dianion of pyrophosphate is just slightly more reactive than the monoanion probably because the second negative charge is not in a position to assist cooperatively in ion-pair formation since it is on the second phosphate center.

The observation that both $H_2PO_4^-$ and H_3PO_4 are reactive nucleophiles has precedent in the study of Ferrer and Sykes[14] with $(NH_3)_5CrOH_2^{3+}$. In the latter case, it was concluded that the product of the ion-pair formation constant and the substitution rate constant is 5.6 times larger for $H_2PO_4^-$ at 25 °C. This is quite similar to the factor of 6.9 observed here with $(H_2O)_5CrCH_2CN^{2+}$. A similar comparison can be made for $H_2PO_2^-$ and H_3PO_2, and the ratios are 2.5 (at 50 °C)[15] and 2.3, respectively. Although differences in ion-pair formation constants would be expected for the two chromium complexes, the similarity in reactivity trends is remarkable and may point to a similar substitution mechanism. It has been argued[16] that anation of $(NH_3)_5CrOH_2^{3+}$ has a mechanism intermediate between I_a and I_d. This interpretation is consistent with the lack of constancy of rate constant with entering group noted above and noted previously[3] for $(H_2O)_5CrCH_2CN^{2+}$.

The rate constants for the second step (k_2, k_2') have been assigned to trans to cis isomerization. It should be noted that this process could be a combination of chelation and ring opening as shown for pyrophosphate in eq 10. The rate constant for ring

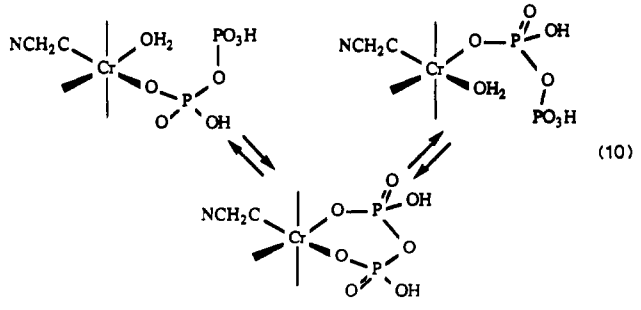

(10)

opening would be expected to be similar to k_{-1}, and therefore the process would be fast on the time scale of the second step. Then the chelate would not appear as an observable intermediate during the reaction.

The observation that $K_{a_1}' \gg [H^+]$ for phosphate (Scheme II) is consistent with previous results on the pentaamminecobalt(III) complex.[17] The fact that $NCCH_2Cr(O_4PH_2)^+$ does not ionize under the acidic conditions of this study is also consistent with the pK_a of 3.5[17] for $(NH_3)_5Co(O_4PH_2)^{2+}$.

The fact that K_{a_2}' (0.12) is slightly smaller than K_{a_1} (0.17) for pyrophosphate (Scheme III) is not surprising, but the apparently much smaller values for K_{a_2}'' and K_{a_3} are noteworthy and have been discussed above. It was suggested that $K_{a_2}'' \approx 0.01$ and $K_{a_3} \leq 0.001$. If this is the case, then the experimental value of $K_{f_2}K_{a_2}''/K_{a_3}$ can be used to estimate that $K_{f_2} \approx 10$ M^{-1}. The latter value is similar to K_f (14.8), and such a similarity also is noted for the $H_2PO_4^-$ and $H_2PO_2^-$ systems. Since $k_3K_{a_3} = 4 \times 10^{-6}$ for pyrophosphate, if $K_{a_3} \approx 0.001$, then it is possible to estimate that $k_3 \approx 4 \times 10^{-3}$ for loss of the alkyl group in Scheme III. It is reasonable to expect the latter value to be larger than k_3' because of the more negative charge and greater ligand basicity in $NCH_2CCr(H_2P_2)_2^{2-}$ compared to those in $NCH_2CCr(H_2P_2)(H_3P_2)^-$ and because the former is more likely to be chelated. This analysis shows that the suggested magnitudes of K_{a_2}'' and K_{a_3} do not yield unreasonable values for other parameters.

It is difficult to comment on the rate constants for loss of the alkyl group (k_3) because values under reasonably acidic conditions are only available for phosphate and pyrophosphate. The process has been observed qualitatively with hypophosphite[2] and oxalate[3] on a much longer time scale, at higher pH with acetate[18] and with EDTA type ligands.[19] It may be that the protonated oxyanion ligands provide some intramolecular assistance for loss of the alkyl group as has been suggested[19] to explain the higher reactivity of EDTA, which has a free $-CO_2H$ group. From the standpoint of preparative applications, it is convenient that the alkyl group is lost relatively easily if one wishes to make aquachromium(III) complexes.

Experimental Section

Materials. Solutions of $(H_2O)_5CrCH_2CN^{2+}$ were prepared as described previously.[20] $NaH_2PO_4 \cdot H_2O$, $Na_4P_2O_7 \cdot 10H_2O$, and $NaClO_4 \cdot H_2O$ were used as supplied (Fisher). In order to maintain the required ionic strength and acidity, it was necessary to prepare some pyrophosphate solutions from $Na_2H_2P_2O_7$, which was prepared by standard methods.[21]

Ion-exchange separations of the reaction products were done in a cold room. The reaction mixtures were diluted with cold water to give an ionic strength of ≤0.1 M before loading them on the ion-exchange resin.

Phosphate and pyrophosphate were determined by the method described by Douglas and Field,[7] which involves formation of a blue phosphomolybdate complex. The chromium(III) phosphate and pyrophosphate complexes were decomposed by heating the samples in acidic solution in the presence of molybdate for 3–4 h on a steam bath. The solution was cooled to ambient temperature before the ascorbate was added. If the samples contained mercury(II), it was necessary to add 2–3 drops of concentrated HCl before the molybdate was added, and then the sample was heated as before.

Chromium was determined as chromate after oxidation in alkaline hydrogen peroxide as described previously.[20]

Instrumentation. The stopped-flow and spectrophotometer systems are described elsewhere.[2,22]

Acknowledgment. We acknowledge the financial support of the Natural Sciences and Engineering Research Council of Canada.

(14) Ferrer, M.; Sykes, A. G. *Inorg. Chem.* **1979**, *18*, 3345.
(15) Martinez, M.; Sykes, A. G. *Inorg. Chim. Acta* **1983**, *69*, 123.
(16) Castillo, S.; Sykes, A. G. *Inorg. Chem.* **1984**, *23*, 1049.
(17) Lincoln, S. F.; Jayne, J.; Hunt, J. P. *Inorg. Chem.* **1969**, *8*, 2267.
(18) Ogino, H.; Shimura, M.; Tanaka, N. *J. Chem. Soc., Chem. Commun.* **1983**, 1063.
(19) Shimura, M.; Ogino, H.; Tanaka, N. *Chem. Lett.* **1985**, 149.
(20) Kupferschmidt, W.; Jordan, R. B. *J. Am. Chem. Soc.* **1984**, *106*, 991.
(21) Bell, R. N. *Inorg. Synth.* **1950**, *3*, 99.
(22) Pinnell, D.; Jordan, R. B. *Inorg. Chem.* **1979**, *18*, 3595.